Proposal of a Novel Lattice Knot Manipulator

Ravi Tripathi and Rama Krishna K

Abstract This study integrates kinematic linkage theory with knot theory by modeling non-self-intersecting closed chains as piecewise-linear embeddings. A trefoil knot is represented as a multi-DOF spatial closed-loop manipulator composed entirely of revolute joints. The manipulator consists of an assembly of rigid segments arranged within a cubic lattice. A screw-theoretic framework is employed to investigate the motion behaviour of end-effector of the lattice knot manipulator (LKM) by analyzing the resulting twists under various joint-rate inputs.

1 Introduction

The design of closed kinematic chains is a long-standing area of research in mechanisms and robotics. Although significant progress has been made in the study of multi-degrees of freedom (DOF) planar closed-loop mechanisms [6, 8], research on multi-DOF spatial closed-loop mechanisms remains limited. In spatial manipulators, often the focus is on serial, in-parallel, and hybrid architectures. The reason for less focus on multi-DOF spatial closed-loop mechanisms could be the relatively large space their embodiments may occupy. Usually, multi-DOF planar and spatial mechanisms are often designed as single loop or multi-loop arrangements.

R. Tripathi
Department of Mechanical Engineering, Indian Institute of Technology Delhi, New Delhi - 110 016, India
e-mail: Ravi.Tripathi@mech.iitd.ac.in

R. Krishna K
Department of Mechanical Engineering, Indian Institute of Technology Delhi, New Delhi - 110 016, India

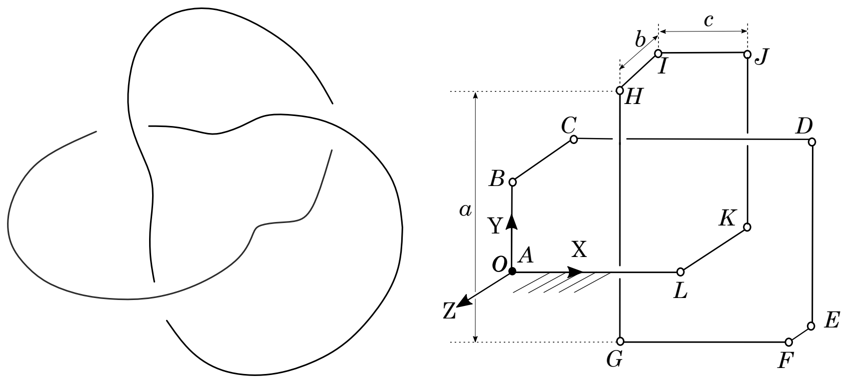

(a) (b)

Fig. 1: (a) Trefoil knot (b) 12-stick trefoil lattice knot

In this paper, we use the new idea that a closed-loop linkage can be designed in a knotted configuration wherein it forms a non-self-intersecting closed spatial chain. Basically, we are inspired from the entities called *knots* in mathematics. In topology, a knot K is defined as a smooth embedding of the unit circle S^1 in three-dimensional Euclidean space $\mathbb{R}^3$ [2]. From a mechanical perspective, a knot may be viewed as a closed-loop kinematic chain in which the spatial curve is idealized as a sequence of rigid links connected by joints, typically of revolute type. *Polygonal knots* provide piecewise-linear approximations of such embeddings using straight segments and allow discrete analysis [3]. A further restriction leads to *lattice knots*, composed of straight line segments that run only along the grid directions (X,Y,Z axes). Lattice knot is a knot embedded in the cubic lattice (the infinite 3D grid of points with integer coordinates) [7,9]. The lattice stick number $s_L(K)$ is the minimum number of line segments required to realize a given lattice knot; for example $s_L(3_1) = 12$ for the *trefoil knot* [1,10,11] shown in Fig. 1(a).

In this work, a trefoil lattice knot is proposed to be modeled as multi-DOF spatial closed-loop manipulator by interpreting it as an assembly of straight segments arranged on a cubic grid. The geometry and mobility of this novel Lattice Knot Manipulator (LKM) is discussed in section 2. The velocity analysis using screw theory is detailed in section 3 of the paper.

2 Architecture, Geometry, and Mobility of LKM

A knot can be realized kinematically as a closed-loop spatial manipulator, such a realization must satisfy specific geometric conditions to constitute a knotted linkage. The Fáry–Milnor theorem [4] states that a smooth closed curve in three-dimensional space forms a nontrivial knot only if its *total curvature* is at least 4π; if the total curvature is less than or equal to 4π, the curve is necessarily an *unknot*. An analogous result holds for closed discrete linkages, which can realise a nontrivial knot only when their total turning angle exceeds 4π . For the case illustrated in Fig. 1(b) and Fig. 2, the total turning angle equals 6π, and hence the given configuration satisfies the knot condition.

Fig. 1(a) illustrates the trefoil knot, defined as the simplest non-trivial, non-self-intersecting closed curve within a three-dimensional spatial domain ($\mathbb{R}^3$). Its corresponding lattice discretization is depicted in Fig. 1(b), modelled as a sequence of piecewise linear segments—referred to as sticks—interconnected at discrete joints. The polygonal structure shown in Fig. 1(b) is characterized by a specific planar alignment: every three consecutive joints are coplanar. For instance, joints $\{A, B, C\}$ define a frontal plane, while $\{B, C, D\}$ and $\{C, D, F\}$ occupy horizontal and lateral-vertical planes, respectively. This geometric constraint is consistently applied throughout the remaining segments of the lattice.

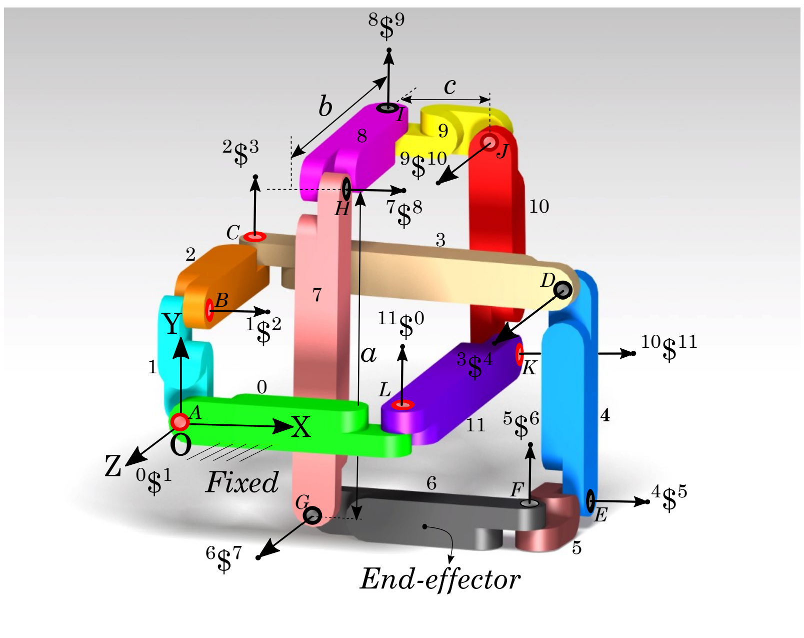

Fig. 2: Trefoil type LKM.

The spatial closed-loop manipulator illustrated in Fig. 2 features an architecture derived from the trefoil knotted lattice configuration shown in Fig. 1(b), with every interconnection at each joint achieved through a revolute pair. The assembly has 12 joints, labeled $\{A, B, C, \ldots, L\}$, and a sequence of 12 interconnected link segments numbered $\{0, 1, \ldots, 11\}$, with link 0 fixed and link 6 designated as the end-effector of the spatial manipulator. A space fixed frame {X,Y,Z} is attached to the joint A. The manipulator shown in Fig. 2 incorporates three distinct link lengths: links $\{GH, CD, LK\}$ measure a units; $\{AB, FE, IJ\}$ measure c units; and the remaining links $\{AL, BC, HI, JK, DE\}$ measure b units.

The mobility (M) of the lattice (box-shaped) spatial linkage shown in Fig. 2, comprising $N = 12$ rigid links and $j = 12$ revolute joints, is determined using the Grübler-Kutzbach formula for spatial mechanisms, where f_i represents the number of degrees of freedom associated with the ith joint.

$$M = 6(N - 1 - j) + \sum_{i=1}^{j}(f_i) = 6 \tag{1}$$

This implies that the mechanism possesses six independent degrees of freedom, and therefore requires six independent inputs for complete control. Accordingly, the trefoil linkage consists of twelve joints, six of which are active while the remaining six are passive. As illustrated in Fig. 2, the active joint set includes $\{A, B, C, J, K, L\}$ (marked red), with all other revolute joints remaining passive.

3 Velocity Analysis

We now analyze the first-order instantaneous motion characteristics of LKM in the *home configuration* shown in Fig. 2. Using screw theory [5], the screws corresponding to the revolute pairs are given by:

$${}^{i}\$^{i+1} = {}_{i}\dot{\theta}_{i+1} \begin{bmatrix} {}^{i}S^{i+1} \\ {}^{i}S_{O}^{i+1} \end{bmatrix} \tag{2}$$

where ${}^{i}S^{i+1}$ represents the unit direction vector or unit angular velocity along each joint axis and ${}^{i}S_{O}^{i+1}$ is the line moment of the axis about reference point O. The loop closure equation for the lattice knot linkage in terms of screw coordinates, shown in Fig. 2 can be written as:

$$\begin{aligned}&{}_{0}\dot{\theta}_{1}\ {}^{0}\$^{1} +_{1} \dot{\theta}_{2}\ {}^{1}\$^{2} +_{2} \dot{\theta}_{3}\ {}^{2}\$^{3} +_{3} \dot{\theta}_{4}\ {}^{3}\$^{4} +_{4} \dot{\theta}_{5}\ {}^{4}\$^{5} +_{5} \dot{\theta}_{6}\ {}^{5}\$^{6} \\ &+_{6} \dot{\theta}_{7}\ {}^{6}\$^{7} +_{7} \dot{\theta}_{8}\ {}^{7}\$^{8} +_{8} \dot{\theta}_{9}\ {}^{8}\$^{9} +_{9} \dot{\theta}_{10}\ {}^{9}\$^{10} +_{10} \dot{\theta}_{11}\ {}^{10}\$^{11} +_{11} \dot{\theta}_{0}\ {}^{11}\$^{0} = 0\end{aligned} \tag{3}$$

Where ${}^{i}\$^{i+1}$ represents, the relative *twist* of link $i+1$ w.r.t. link i and ${}_{i}\dot{\theta}_{i+1}$ amplitude of the angular velocity.

The directions of the six joint axes, expressed in the fixed reference frame shown in Fig. 2, are given by:

$$
\begin{aligned}
&{}^{0}S^{1} = \{0,0,1\}^T, \quad {}^{1}S^{2} = \{1,0,0\}^T, \quad {}^{2}S^{3} = \{0,1,0\}^T \\
&{}^{3}S^{4} = \{0,0,1\}^T, \quad {}^{4}S^{5} = \{1,0,0\}^T, \quad {}^{5}S^{6} = \{0,1,0\}^T \\
&{}^{6}S^{7} = \{0,0,1\}^T, \quad {}^{7}S^{8} = \{1,0,0\}^T, \quad {}^{8}S^{9} = \{0,1,0\}^T \\
&{}^{9}S^{10} = \{0,0,1\}^T, \quad {}^{10}S^{11} = \{1,0,0\}^T, \quad {}^{11}S^{0} = \{0,1,0\}^T
\end{aligned} \tag{4}
$$

Then the moment of the line along the ith joint w.r.t to the fixed reference frame O is given by:

$$
\begin{aligned}
&{}^{0}S^{1}_{O} = \{0,0,0\}^T, \quad {}^{1}S^{2}_{O} = \{0,0,-c\}^T, \quad {}^{2}S^{3}_{O} = \{b,0,0\}^T \\
&{}^{3}S^{4}_{O} = \{c,-a,0\}^T, \quad {}^{4}S^{5}_{O} = \{0,-b,(b-c)\}^T, \quad {}^{5}S^{6}_{O} = \{(b-c),0,a\}^T \\
&{}^{6}S^{7}_{O} = \{-(a-b),-(a-b),0\}^T, \quad {}^{7}S^{8}_{O} = \{0,-(b-c),-b\}^T, \\
&{}^{8}S^{9}_{O} = \{a,0,(b-c)\}^T \quad {}^{9}S^{10}_{O} = \{b,-b,0\}^T, \\
&{}^{10}S^{11}_{O} = \{0,-a,0\}^T, \quad {}^{11}S^{0}_{O} = \{0,0,b\}^T
\end{aligned} \tag{5}
$$

Eq. (3) can now be written in matrix form as

$$[\boldsymbol{J}]_{6\times 12}[\dot{\boldsymbol{\theta}}]_{12\times 1} = 0 \tag{6}$$

Here, $\boldsymbol{J}$ is the 6×12 Jacobian matrix expressed in terms of the unitized screw coordinates of the system, with its columns corresponding to the Plücker coordinates of the revolute joints

$$\boldsymbol{J} = \begin{bmatrix} {}^{0}\$^{1} & {}^{1}\$^{2} & {}^{2}\$^{3} & {}^{3}\$^{4} & {}^{4}\$^{5} & {}^{5}\$^{6} & {}^{6}\$^{7} & {}^{7}\$^{8} & {}^{8}\$^{9} & {}^{9}\$^{10} & {}^{10}\$^{11} & {}^{11}\$^{0} \end{bmatrix} \tag{7}$$

and $\dot{\boldsymbol{\theta}}$ denotes the vector of joint velocities, given by

$$\dot{\boldsymbol{\theta}} = \begin{bmatrix} {}_{0}\dot{\theta}_{1} & {}_{1}\dot{\theta}_{2} & {}_{2}\dot{\theta}_{3} & {}_{3}\dot{\theta}_{4} & {}_{4}\dot{\theta}_{5} & {}_{5}\dot{\theta}_{6} & {}_{6}\dot{\theta}_{7} & {}_{7}\dot{\theta}_{8} & {}_{8}\dot{\theta}_{9} & {}_{9}\dot{\theta}_{10} & {}_{10}\dot{\theta}_{11} & {}_{11}\dot{\theta}_{0} \end{bmatrix}^T \tag{8}$$

Eq. (6) can also be written in terms of partitioned form in terms of passive and active joint rates as:

$$\boldsymbol{J}\dot{\boldsymbol{\theta}} = \boldsymbol{J}_a\dot{\boldsymbol{\theta}}_a + \boldsymbol{J}_p\dot{\boldsymbol{\theta}}_p = 0 \tag{9}$$

If $\boldsymbol{J_p}$ is invertible, then the passive joint rates are obtained as:

$$\dot{\boldsymbol{\theta}}_p = -\boldsymbol{J}_p{}^{-1}\boldsymbol{J}_a\dot{\boldsymbol{\theta}}_a \tag{10}$$

This configuration ensures that the passive joint motions are inherently constrained by the mechanism's geometry. Here, $\dot{\boldsymbol{\theta}}_{\boldsymbol{p}}$ and $\dot{\boldsymbol{\theta}}_{\boldsymbol{a}}$ denote the joint rates for the passive and active joints, respectively, while $\boldsymbol{J_p}$ and $\boldsymbol{J_a}$ represent the corresponding 6×6 Jacobian matrices. Given that the first three and last three joints relative to fixed link 0 are actuated with the intervening joints remaining passive. The passive joint rates can be derived using Eq. (9) as follows:

$$\underbrace{\begin{bmatrix} {}^{0}\$^{1} & {}^{1}\$^{2} & {}^{2}\$^{3} & {}^{9}\$^{10} & {}^{10}\$^{11} & {}^{11}\$^{0} \end{bmatrix}}_{J_a} \underbrace{\begin{bmatrix} {}_{0}\dot{\theta}_{1} \\ {}_{1}\dot{\theta}_{2} \\ {}_{2}\dot{\theta}_{3} \\ {}_{9}\dot{\theta}_{10} \\ {}_{10}\dot{\theta}_{11} \\ {}_{11}\dot{\theta}_{0} \end{bmatrix}}_{\dot{\theta}_a} + \underbrace{\begin{bmatrix} {}^{3}\$^{4} & {}^{4}\$^{5} & {}^{5}\$^{6} & {}^{6}\$^{7} & {}^{7}\$^{8} & {}^{8}\$^{9} \end{bmatrix}}_{J_p} \underbrace{\begin{bmatrix} {}_{3}\dot{\theta}_{4} \\ {}_{4}\dot{\theta}_{5} \\ {}_{5}\dot{\theta}_{6} \\ {}_{6}\dot{\theta}_{7} \\ {}_{7}\dot{\theta}_{8} \\ {}_{8}\dot{\theta}_{9} \end{bmatrix}}_{\dot{\theta}_p} = 0.$$

In other words,

$$\begin{bmatrix} 0 & 1 & 0 & 0 & 1 & 0 \\ 0 & 0 & 1 & 0 & 0 & 1 \\ 1 & 0 & 0 & 1 & 0 & 0 \\ 0 & 0 & b & b & 0 & 0 \\ 0 & 0 & 0 & -b & -a & 0 \\ 0 & -c & 0 & 0 & 0 & b \end{bmatrix} \begin{bmatrix} {}_{0}\dot{\theta}_{1} \\ {}_{1}\dot{\theta}_{2} \\ {}_{2}\dot{\theta}_{3} \\ {}_{9}\dot{\theta}_{10} \\ {}_{10}\dot{\theta}_{11} \\ {}_{11}\dot{\theta}_{0} \end{bmatrix} + \begin{bmatrix} 0 & 1 & 0 & 0 & 1 & 0 \\ 0 & 0 & 1 & 0 & 0 & 1 \\ 1 & 0 & 0 & 1 & 0 & 0 \\ c & 0 & (b-c) & -(a-b) & 0 & a \\ -a & -b & 0 & -(a-b) & -(b-c) & 0 \\ 0 & (b-c) & a & 0 & -b & (b-c) \end{bmatrix} \begin{bmatrix} {}_{3}\dot{\theta}_{4} \\ {}_{4}\dot{\theta}_{5} \\ {}_{5}\dot{\theta}_{6} \\ {}_{6}\dot{\theta}_{7} \\ {}_{7}\dot{\theta}_{8} \\ {}_{8}\dot{\theta}_{9} \end{bmatrix} = 0.$$

Therefore,

$$\begin{bmatrix} {}_{1}\dot{\theta}_{2} +_{10} \dot{\theta}_{11} \\ {}_{2}\dot{\theta}_{3} +_{11} \dot{\theta}_{0} \\ {}_{0}\dot{\theta}_{1} +_{9} \dot{\theta}_{10} \\ ({}_{2}\dot{\theta}_{3} +_{9} \dot{\theta}_{10})b \\ -({}_{9}\dot{\theta}_{10})b - ({}_{10}\dot{\theta}_{11})a \\ -({}_{1}\dot{\theta}_{2})c + ({}_{11}\dot{\theta}_{0})b \end{bmatrix} + \begin{bmatrix} 0 & 1 & 0 & 0 & 1 & 0 \\ 0 & 0 & 1 & 0 & 0 & 1 \\ 1 & 0 & 0 & 1 & 0 & 0 \\ c & 0 & (b-c) & -(a-b) & 0 & a \\ -a & -b & 0 & -(a-b) & -(b-c) & 0 \\ 0 & (b-c) & a & 0 & -b & (b-c) \end{bmatrix} \begin{bmatrix} {}_{3}\dot{\theta}_{4} \\ {}_{4}\dot{\theta}_{5} \\ {}_{5}\dot{\theta}_{6} \\ {}_{6}\dot{\theta}_{7} \\ {}_{7}\dot{\theta}_{8} \\ {}_{8}\dot{\theta}_{9} \end{bmatrix} = 0. \tag{11}$$

The inverse of the $\boldsymbol{J_p}$ from Eq.(11) is given by

$$\boldsymbol{J_p}^{-1} = \begin{pmatrix} \frac{2b^2-2bc+c^2}{\Delta} & \frac{-ac-bc+c^2}{\Delta} & \frac{2ab-2b^2}{\Delta} & \frac{c}{\Delta} & \frac{2b-c}{\Delta} & \frac{c}{\Delta} \\ \frac{-ab+ac-2bc+c^2}{\Delta} & \frac{ab+b^2-bc}{\Delta} & \frac{-a^2+ab-ac+bc}{\Delta} & \frac{-b}{\Delta} & \frac{-a+b-c}{\Delta} & \frac{-b}{\Delta} \\ \frac{2b^2-2bc+c^2}{\Delta} & \frac{-2ab^2+ac^2+b^2c-2bc^2+c^3}{\det(A)} & \frac{2a^2b-a^2c-2ab^2+3abc-ac^2-2b^2c+bc^2}{\det(A)} & \frac{2b^2-bc}{\det(A)} & \frac{2b-c}{\Delta} & \frac{c}{\Delta} \\ \frac{-2b^2+2bc-c^2}{\Delta} & \frac{ac+bc-c^2}{\Delta} & \frac{-2ab+ac+c^2}{\Delta} & \frac{-c}{\Delta} & \frac{-2b+c}{\Delta} & \frac{-c}{\Delta} \\ \frac{ab-2b^2+2bc}{\Delta} & \frac{-ab-b^2+bc}{\Delta} & \frac{a^2-ab+ac-bc}{\Delta} & \frac{b}{\Delta} & \frac{a-b+c}{\Delta} & \frac{b}{\Delta} \\ \frac{-2b^2+2bc-c^2}{\Delta} & \frac{a^2c-abc+ac^2+2b^3-3b^2c+bc^2}{\det(A)} & \frac{-2a^2b+a^2c+2ab^2-3abc+ac^2+2b^2c-bc^2}{\det(A)} & \frac{-2b^2+bc}{\det(A)} & \frac{-2b+c}{\Delta} & \frac{-c}{\Delta} \end{pmatrix} \tag{12}$$

where $\Delta = ac - 2b^2 + c^2$ and $\det(A) = a^2c - 2ab^2 - abc + 2ac^2 + 2b^3 - 2b^2c - bc^2 + c^3$. The passive joint rates $\dot{\boldsymbol{\theta}}_p$ are given as

$$
\dot{\boldsymbol{\theta}}_p = -\begin{pmatrix}
\frac{2({}_0\dot{\theta}_1+{}_9\dot{\theta}_{10})(ab-b^2)}{\sigma_{15}} - \sigma_6 + \frac{c\sigma_1}{\sigma_{15}} - \sigma_3 + \sigma_2 + \sigma_{11} \\
\sigma_5 - \frac{b\sigma_1}{\sigma_{15}} - \sigma_{10} - \frac{({}_1\dot{\theta}_2+{}_{10}\dot{\theta}_{11})(ab-ac+2bc-c^2)}{\sigma_{15}} + \sigma_9 + \sigma_7 \\
\frac{c\sigma_1}{\sigma_{15}} - \sigma_3 + \sigma_2 - \frac{({}_2\dot{\theta}_3+{}_{11}\dot{\theta}_0)(b^2c-\sigma_{16}-2bc^2+c^3+ac^2)}{\sigma_{13}} - \sigma_8 + \sigma_4 \\
\sigma_6 - \frac{c\sigma_1}{\sigma_{15}} + \sigma_3 - \sigma_2 + \frac{({}_0\dot{\theta}_1+{}_9\dot{\theta}_{10})(c^2+ac-2ab)}{\sigma_{15}} - \sigma_{11} \\
\sigma_{10} + \frac{({}_1\dot{\theta}_2+{}_{10}\dot{\theta}_{11})(ab+2bc-2b^2)}{\sigma_{15}} + \frac{b\sigma_1}{\sigma_{15}} - \sigma_5 - \sigma_9 - \sigma_7 \\
\sigma_3 - \frac{({}_2\dot{\theta}_3+{}_{11}\dot{\theta}_0)(a^2c-abc+ac^2+2b^3-3b^2c+bc^2)}{\sigma_{13}} - \frac{c\sigma_1}{\sigma_{15}} - \sigma_2 + \sigma_8 - \sigma_4
\end{pmatrix} \tag{13}
$$

where

$$
\sigma_1 = b\ {}_{11}\dot{\theta}_0 - c\ {}_1\dot{\theta}_2, \quad \sigma_2 = \frac{({}_1\dot{\theta}_2 +_{10} \dot{\theta}_{11})(2b^2-2bc+c^2)}{\sigma_{15}}, \quad \sigma_3 = \frac{\sigma_{14}(2b-c)}{\sigma_{15}}
$$

$$
\sigma_4 = \frac{({}_0\dot{\theta}_1 +_9 \dot{\theta}_{10})(2b-c)\sigma_{12}}{\sigma_{13}}, \quad \sigma_5 = \frac{({}_0\dot{\theta}_1 +_9 \dot{\theta}_{10})\sigma_{12}}{\sigma_{15}}
$$

$$
\sigma_6 = \frac{({}_2\dot{\theta}_3 +_{11} \dot{\theta}_0)(ac+bc-c^2)}{\sigma_{15}}, \quad \sigma_7 = \frac{({}_2\dot{\theta}_3 +_{11} \dot{\theta}_0)(ab-bc+b^2)}{\sigma_{15}}
$$

$$
\sigma_8 = \frac{b^2({}_2\dot{\theta}_3 +_9 \dot{\theta}_{10})(2b-c)}{\sigma_{13}}, \quad \sigma_9 = \frac{\sigma_{14}(a-b+c)}{\sigma_{15}}
$$

$$
\sigma_{10} = \frac{b^2({}_2\dot{\theta}_3 +_9 \dot{\theta}_{10})}{\sigma_{15}}, \quad \sigma_{11} = \frac{bc({}_2\dot{\theta}_3 +_9 \dot{\theta}_{10})}{\sigma_{15}}, \quad \sigma_{12} = ab - ac + bc - a^2
$$

$$
\sigma_{13} = -a^2c + \sigma_{16} + abc - 2ac^2 - 2b^3 + 2b^2c + bc^2 - c^3
$$

$$
\sigma_{14} = a\ {}_{10}\dot{\theta}_{11} + b\ {}_9\dot{\theta}_{10}, \quad \sigma_{15} = -2b^2 + c^2 + ac, \quad \sigma_{16} = 2ab^2
$$

3.1 Numerical Cases

The link lengths are assumed as $\{GH, CD, LK\} = a = 150$ units, $\{AB, FE, IJ\} = c = 50$ units, and $\{AI, BC, HI, JK, DE\} = b = 100$ units. Having obtained the generalized joint rates and specified the link dimensions, the following cases examine the resulting motion characteristics of the end effector.

Case 1: When three simultaneous active joint rates on the left and right sides of the fixed link are each assigned a value of 1 rad/sec. Finally, the passive joint rates can be obtained from Eq. (13) as

$$
\left[{}_3\dot{\theta}_4 \ \ {}_4\dot{\theta}_5 \ \ {}_5\dot{\theta}_6 \ \ {}_6\dot{\theta}_7 \ \ {}_7\dot{\theta}_8 \ \ {}_8\dot{\theta}_9\right]^T = \left[0.0, -1.0, 0.0, -2.0, -1.0, -2.0\right]^T \tag{14}
$$

Now that the joint rates of both the passive and active joints are known, the twist of the end-effector with respect to the fixed reference frames O can be expressed as

$$
\mathbf{{}^0\$^6} =_0 \dot{\theta}_1\ {}^0\$^1 +_1 \dot{\theta}_2\ {}^1\$^2 +_2 \dot{\theta}_3\ {}^2\$^3 +_3 \dot{\theta}_4\ {}^3\$^4 +_4 \dot{\theta}_5\ {}^4\$^5 +_5 \dot{\theta}_6\ {}^5\$^6 \tag{15}
$$

Eq. (15) can also be written in matrix form as

$$\mathbf{{}^{0}\$^{6}} = \begin{bmatrix} 0 & 1 & 0 & 0 & 1 & 0 \\ 0 & 0 & 1 & 0 & 0 & 1 \\ 1 & 0 & 0 & 1 & 0 & 0 \\ 0 & 0 & b & c & 0 & (b-c) \\ 0 & 0 & 0 & -a & -b & 0 \\ 0 & -c & 0 & 0 & (b-c) & a \end{bmatrix} \begin{bmatrix} {}_0\dot{\theta}_1 \\ {}_1\dot{\theta}_2 \\ {}_2\dot{\theta}_3 \\ {}_3\dot{\theta}_4 \\ {}_4\dot{\theta}_5 \\ {}_5\dot{\theta}_6 \end{bmatrix} = \begin{bmatrix} 0 & 1 & 0 & 0 & 1 & 0 \\ 0 & 0 & 1 & 0 & 0 & 1 \\ 1 & 0 & 0 & 1 & 0 & 0 \\ 0 & 0 & 100 & 50 & 0 & 50 \\ 0 & 0 & 0 & -150 & -100 & 0 \\ 0 & -50 & 0 & 0 & 50 & 150 \end{bmatrix} \begin{bmatrix} {}_0\dot{\theta}_1 \\ {}_1\dot{\theta}_2 \\ {}_2\dot{\theta}_3 \\ {}_3\dot{\theta}_4 \\ {}_4\dot{\theta}_5 \\ {}_5\dot{\theta}_6 \end{bmatrix} \tag{16}$$

Hence, the end-effector twist ($\mathbf{{}^{0}\$^{6}}$) reduces to [0,1,1;100,100,-100]. The amplitude of the twist is $\sqrt{2}$ rad/sec and the associated pitch in this case is zero.

Observation 1: The twist exhibits a zero-pitch screw, indicating that the end-effector undergoes pure rotation about its screw axis.

Case 2: The three active joint rates are set to 1 rad/sec on the left side and 2 rad/sec on the right side of the fixed link. In this case , Eq. (13) yields the passive joint rates as

$$\begin{bmatrix} {}_3\dot{\theta}_4 & {}_4\dot{\theta}_5 & {}_5\dot{\theta}_6 & {}_6\dot{\theta}_7 & {}_7\dot{\theta}_8 & {}_8\dot{\theta}_9 \end{bmatrix}^T = \begin{bmatrix} -1.5, & -1.0, & -1.5, & -1.5, & -2.0, & -1.5 \end{bmatrix}^T \tag{17}$$

Hence, the end-effector twist ($\mathbf{{}^{0}\$^{6}}$) from Eq. (16) is obtained as

$$\mathbf{{}^{0}\$^{6}} = \begin{bmatrix} 0, & -0.5, & -0.5; & -50, & 325, & -325 \end{bmatrix} \tag{18}$$

In this case, the amplitude of the twist is $1/\sqrt{2}$ rad/sec and the associated pitch is zero.

Observation 2: In this case as well, the end-effector link undergoes pure rotation.

Case 3: When the values of all active joint rates on the left and right sides of the fixed link are different. Let the active joint rates be $\begin{bmatrix} {}_0\dot{\theta}_1 & {}_1\dot{\theta}_2 & {}_2\dot{\theta}_3 & {}_9\dot{\theta}_{10} & {}_{10}\dot{\theta}_{11} & {}_{11}\dot{\theta}_0 \end{bmatrix}^T = [1, 2, 3, 4, 5, 6]$ rad/sec. The corresponding passive joints rates (in rad/sec) are given by

$$\begin{bmatrix} {}_3\dot{\theta}_4 & {}_4\dot{\theta}_5 & {}_5\dot{\theta}_6 & {}_6\dot{\theta}_7 & {}_7\dot{\theta}_8 & {}_8\dot{\theta}_9 \end{bmatrix}^T = \begin{bmatrix} -6.5, & 2.0, & -10.5, & 1.5, & -9.0, & 1.50 \end{bmatrix}^T \tag{19}$$

As a result, the end-effector twist obtained from Eq. (16) is

$$\mathbf{{}^{0}\$^{6}} = \begin{bmatrix} 4.00, & -7.50, & -5.50; & -550, & 775, & -1575 \end{bmatrix} \tag{20}$$

with amplitude 10.12 rad/sec and a non-zero pitch ($h \approx 65$ units)
Observation 3: In this case, the end-effector is in a general screw motion.

4 Closure

This work has presented an architecture of a new 6-DOF closed-loop manipulator inspired from a lattice knot. The velocity analysis of the LKM has revealed that the end-effector of the manipulator is capable of performing general spatial motion. Even though the workspace of the end-effector of such a manipulator is small, it may have potential applications in the design of precision devices and medical surgeries. Hardware realization of a LKM should address the issues of singularities, link interference, and joint limits. An extension to the present work can explore more complex knot geometries.

Acknowledgements The authors would like to express their sincere gratitude to Prof. Dibakar Sen, IISc Bangalore, for his inspiration and encouragement in exploring the potential applications of knot theory in Mechanical Engineering.

References

1. Adams, C., Chu, M., Crawford, T., Jensen, S., Siegel, K., Zhang, L.: Stick index of knots and links in the cubic lattice. Journal of Knot Theory and Its Ramifications **21**(05), 1250,041 (2012)
2. Adams, C.C.: The knot book: an elementary introduction to the mathematical theory of knots. American Mathematical Soc. (2004)
3. Armstrong, M.A.: Basic topology. Springer Science & Business Media (2013)
4. Chirikjian, G.S., Kyatkin, A.B.: Engineering applications of noncommutative harmonic analysis: with emphasis on rotation and motion groups. CRC press (2000)
5. Davidson, J., Hunt, K.: Robots and Screw Theory: Applications of kinematics and statics to robotics. Oxford University Press (2004)
6. Di Gregorio, R.: Kinematic analysis of multi-dof planar mechanisms via velocity-coefficient vectors and acceleration-coefficient jacobians. Mechanism and Machine Theory **142**, 103,617 (2019)
7. Diao, Y.: Minimal knotted polygons on the cubic lattice. Journal of Knot Theory and its Ramifications **2**(04), 413–425 (1993)
8. Funke, L.W., Schmiedeler, J.P., Zhao, K.: Design of planar multi-degree-of-freedom morphing mechanisms. Journal of Mechanisms and Robotics **7**(1) (2015)
9. Hinojosa, G., Verjovsky, A., Verjovsky Marcotte, C.: Cubulated moves and discrete knots. Journal of knot theory and its ramifications **22**(14), 1350,079 (2013)
10. Hong, K., No, S., Oh, S.: Upper bound on lattice stick number of knots. In: Mathematical Proceedings of the Cambridge Philosophical Society, vol. 155, pp. 173–179. Cambridge University Press (2013)
11. Huh, Y., Oh, S.: Knots with small lattice stick numbers. Journal of Physics A: Mathematical and Theoretical **43**(26), 265,002 (2010)